AN INVESTIGATION ON ATMOSPHERIC EFFECTS IN AIRBORNE INTERFEROMETRIC SAR DATA

Andreas Danklmayer and Karlus A. C. de Macedo

Microwaves and Radar Institute, German Aerospace Center, DLR,Oberpfaffenhofen, PO Box 1116, D-82230 Wessling, Germany, Email: Andreas.Danklmayer@dlr.de

ABSTRACT

The results of an experiment on atmospheric effects in interferometric SAR data are presented. The main purpose of the experiment was to investigate on the influence of the troposphere on airborne synthetic aperture radar measurements, acquired by DLR's experimental E-SAR system. The analysed data was acquired at L-band. The main idea behind the experiment is to collect data sets at different atmospheric conditions and to compare the measurements by performing a differential interferometric analysis. The main difference between atmospheric conditions on "Day-one" and "Day-two" of acquisition was cloud layer between sensor and illuminated surface, reaching from 750 to 1500 m above sea-level (msl). The sensor altitude was about 3000 m (msl). The test site is located at 580 m (msl). The results of the experiment will be highlighted and an interpretation of the observed differential effects will be given. In a first investigation [1] no pronounced indication of atmospheric effects in L-band interferograms was found. In this contribution, two different techniques, multisquint [6] and Weighted Phase Curvature Autofocus (WPCA) [3], are applied to accurately mitigate residual motion errors allowing for a better interpretation of any possible atmospheric effects.

Key words: SAR, atmospheric effects, tropospheric effects, DInSAR.

1. INTRODUCTION

An atmospheric SAR experiment was conducted in October 2005 at the Microwaves and Radar Institute (HR), DLR - German Aerospace Center, where microwave remote sensing has a long tradition. The main purpose of the experiment was to investigate the influence of the troposphere on airborne-synthetic-aperture-radar measurements, acquired by DLR's experimental E–SAR System. E–SAR is a multi-band airborne SAR system flown on a modified Do 228–212 with high operational flexibility and imaging capabilities.

In the context of space-borne SAR systems, e.g. like ERS-1 and ERS-2 there exist several studies about propagation effects and efforts were spend how to make use of SAR to remotely sense information about the troposphere and to identify related propagation effects [7], [4]. However, no relevant publications could be found for the airborne case and the demand for studies on this subject is motivated primarily to identify error contributions in differential interfermetric airborne imaging.

The main idea behind the experiment presented here was to collect data sets at different atmospheric conditions with an airborne sensor and to compare the measurements by performing a differential interferometric analysis described in more detail in Section 2. At the onset of the experiment design phase, a configuration with pronounced differences between atmospheric conditions on "Day–one"and 'Day–two" of acquisition was sought. Ideally, a heavy thunderstorm (convective cell) on 'Day–one' and a calm and clear–sky 'Day–two' with no precipitation was anticipated and considered best. However the maximum acquisition altitude for E-SAR is restricted to about 4000 m and the danger of corresponding wing icing above the melting band and/or the potential impact of hail stones put constraints on the selection of the respective weather conditions for acquisition.

Thus due to staff and equipment security reasons it was impossible to operate E–SAR during a so called convective weather situation. Instead, conditions with a fog layer between sensor and illuminated surface was finally chosen.

2. DESCRIPTION OF THE EXPERIMENT AND THE ACQUISITION CONDITIONS, ANALYSIS AND DATA PROCESSING

The data acquisition took place at the testsite of Oberpfaffenhofen on the 4^{th} and the 7^{th} of October, 2005. The main acquisiton parameters for the E–SAR system can be found in Tab. 1. The detailed times and additional parameters characterizing the weather conditions are summarized in Tab. 3. On both days two passes with zero baselines were flown where the operating frequency was L-band (Rf-centre frequency 1.3 GHz) and at HH-polarization. The datasets itself were processed using an

extended chirp scaling algorithm [5]. In Fig. 1 the amplitude image of the testite is given.

Furthermore, two different types of residual motion compensation were performed. The 'multsquint technique' according to [6] and the Weighted Phase Curvature Autofocus (WPCA) method due to [3]. "Day–one" was dry with no precipitation; however the sky was fully covered by a closed fog layer approximately reaching from 750 to 1500 m above sea–level, corresponding to a fog-layer thickness of about 750 m. The average height of the test site was around 580 m above sea-level. Temperatures reached 11.3 deg Celsius and humidity was 100 %. Air pressure was quite similar on both days and around 1024 hPa. On "Day–two" clear sky conditions were prevailing during the data takes. Due to the missing fog cover and advanced time of the day temperatures were reaching about 18 deg. Celsius at the time of acquisition; the humidity dropped down to 50 % of "Day–one". Thus four data sets have been acquired allowing for a differential interferometric SAR image generation as in [2]. The main principle behind the analysis is to generate two interferograms using one "master"- and two "slave"- images. The master image stems from the first day of acquisition and the "slave"- images were acquired on the first and on the second day. The respective differential interferogram shall provide insight into any tropospheric changes between acquisitions of "Day–one" and "Day–two", assuming stationary/unchanged topography. For the detailed information on which dataset were used for generation of the differential interferogram see Tab. 2.

3. INTERPRETATION OF THE COHERENCE IMAGES AND THE DIFFERENTIAL INTERFEROGRAMS

In Fig. 2(a) the degree of coherence image is given which was obtained by calculating the degree of coherence between two different passes 'D1' and 'D2' of the 'Day–one'. The values from 0 to 1 are represented by the shades from black (0%) and white (100%). This image is also refered as 'short–term' degree of coherence image.

Furthermore in Fig. 2(b) and Fig. 2(c) the so called 'long–term' degree of coherence images are shown which were obtained using one pass of 'Day–one' and a second pass on 'Day–two'. As can be seen by comparing the images Fig. 2(a) and Fig. 2(b) the degree of coherence is lower in Fig. 2(b) especially for wood–covered areas.

The differential images are given in Fig. 3(a) – Fig. 3(f). The range direction coincides with the horizontal and the azimuth direction is pointing perpendicular. The colour bar provided in Fig. 4 covers the delay and/or displacements with values reaching from -30 mm to a maximum of +30 mm.

Blue coloured zones, especially appearing in the center along the range direction of Fig. 3(a) are due to residual motion errors, indicated by the homogenous spreading along the range direction.

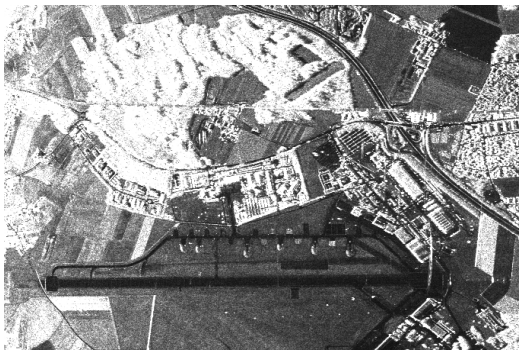

Figure 1. The amplitude image of a specific area of Oberpfaffenhofen, Germany acquired in L–band (HH–polarization)

The suspicious yellow and red regions in the image center of Fig. 3(e) indicates a remaining non-compensatated residual motion error because it does not appear in Fig. 3(c),3(d) and 3(f). The same applies for the top area in yellow also. The blue and remaining yellow zones are basically related to DEM (Digital elevation model) errors rather then the atmosphere due to the strong correlation with the structure. Soil moisture could also explain some differential–interferometric SAR (DInSAR) effects in the agricultural fields. To best of our knowledge, it can be ruled out that these areas are related to atmospheric propagation effects, since they should, if present, have generated a homogenious "phase differences". However this was not observed in the datasets.

The green coloured zones in Fig. 3(c) are dominating and refer to no differential changes or only minor phase changes below the processing accuracy.

4. CONCLUSIONS

As a result of fundamental interest, the experiment revealed that ordinary non-precipitating clouds generally seen do not impair the airborne L–band SAR imaging to any noticeable extent. This conclusion reflects the results obtained form differential images Fig. 3(c) - 3(f) after the motion compensation.

Future studies should investigate SAR imaging at different atmospheric conditions and imaging with higher imaging frequencies, e.g. X-band. The selecetion of future testsites could also include large scale geographic features such as land–sea boundaries or mountainous terrain where possible variations of the water vapor content are expected to be more pronounced.

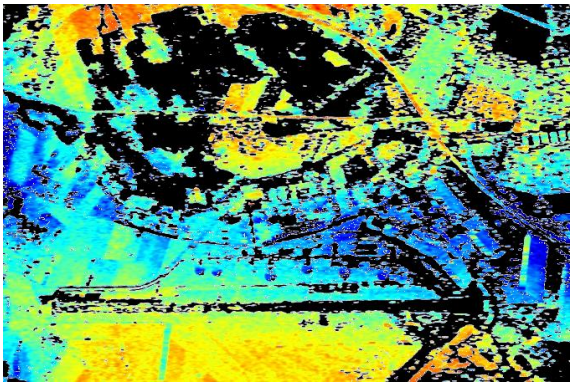

(a) C1 - without motion compensation

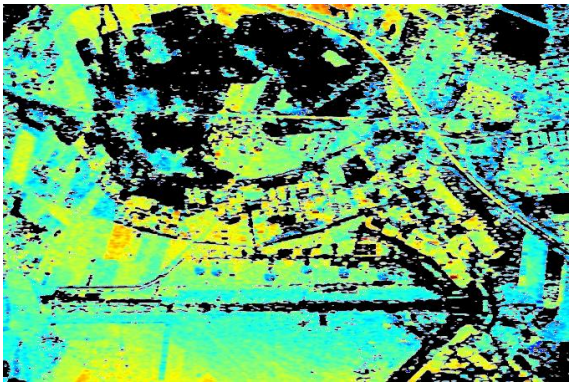

(b) C2 - no motion compensation

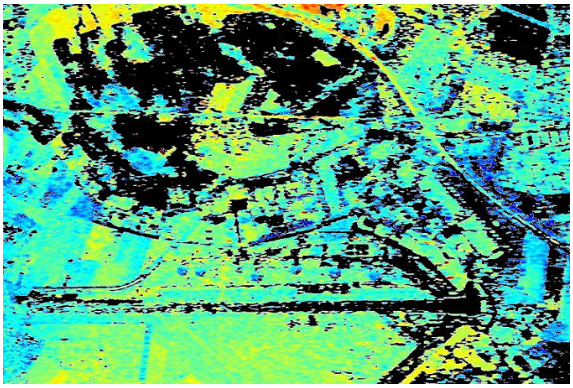

(c) C1 - multisquint

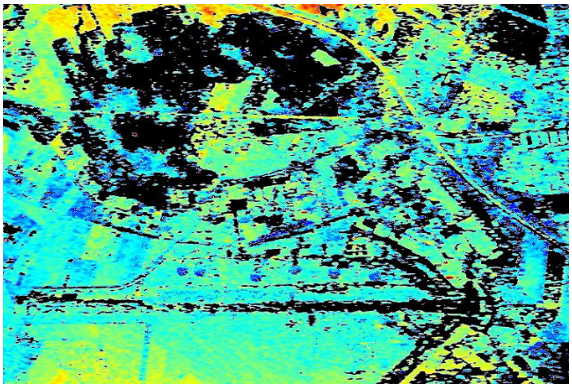

(d) C2 - multisquint

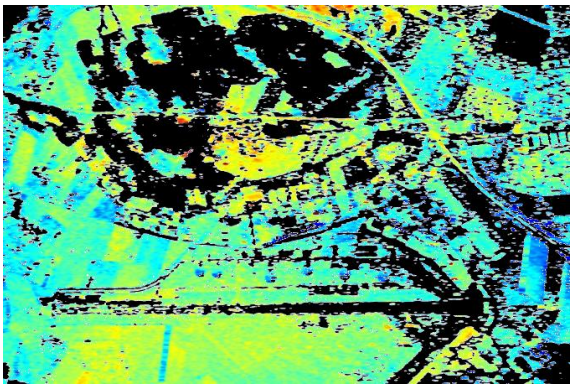

(e) C1 - WPCA

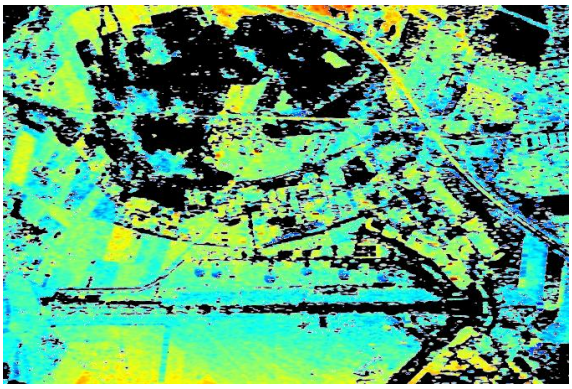

(f) C2 - WPCA

(g) The color bar covers the delay and/or displacements with values reaching from 3 cm to - 3 cm

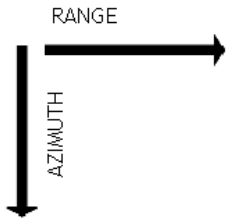

(h) Directions of the coordinates range and azimuth

Figure 3. Differential Interferograms expressing equivalent path differences (mm) between interferograms generated using a common master (recorded on "Day–one") and two different slave images recorded on "Day–one" and "Day–two". The black areas correspond to coherences less than 0.3.

Table 2. The differential combinations show the datatakes that have been used to generate the differential interferograms. The extension: 'no', 'WPCA' and 'Multisquint' refer to the motion compensation technique which has been used to correct for the residual motion errors.

Combinations		Acquisition "Day–one" with cloud cover	Acquisition "Day–two" clear sky
	Master 1	**Slave 1**	**Slave 2**
C1–no	D1	D2	D3
C1–WPCA	D1	D2	D3
C1–Multisquint	D1	D2	D3
C2–no	D1	D2	D4
C2–WPCA	D1	D2	D4
C2–Multisquint	D1	D2	D4

Table 3. Weather and aquisition parameters

Day	**Scene ID**	**Date** [yy.mm.dd]	**Time** [MEZ]	**Air-pressure** [hPa]	**Humidity**	**Temp.** [° C]	**Zentith delay** [m]
Day 1	D1	05.10.04	10:13	954	100 %	11.3	2.32
	D2	05.10.04	10:23	954	100 %	11.3	2.32
Day 2	D3	05.10.07	12:20	952	54 %	18.5	2.292
	D4	05.10.07	12:39	954	53 %	18.5	2.2913

(a) Degree of coherence–image between pass 'D1' on "Day–one" and pass 'D2' on "Day–one", Baseline: vertical 0.1 m and horizontal -9.6 m.)

(b) Degree of coherence–image between pass 'D1' on "Day–one" and pass 'D3' on "Day–two", Baseline: vertical 0.5 m and horizontal 0.1 m.

(c) Degree of coherence–image between pass 'D1' on "Day–one" and pass 'D4' on "Day–two", Baseline: vertical 1.5 m and horizontal -8.7 m.

Figure 2. Degree of coherence–images between two different passes specified under the caption of each individual figure. The values from 0 to 1 are represented by the shades from black (0%) and white (100%)

Table 1. The main acquisition parameter of the E–SAR system for the experiment.

Parameter	**Values**
Wavelength/ Frequency band	0.2305 m / L
Polarization	HH
PRF	400 Hz
Flight velocity	85 m/s
Acquisition height	3770 m
Bandwidth	100 MHz
Range delay	19.5210 μs
Azimuth pixel spacing	0.42 m
Range pixel spacing	1.49 m
Azimuth dimension	2.0 km
Range Dimension	2.5 km

REFERENCES

[1] A. Danklmayer and K. A. C. de Macedob. An experiment on atmospheric effects in airborne interferometric SAR data. In *International Symposium on Antennas and Propagation (ISAP)*, Niigata, Japan, August 2007.

[2] K. A. C. de Macedo, Ch. Andres, and R. Scheiber. On the requirements of SAR processing for airborne differential interferometry. In *Proceedings of International Geoscience and Remote Sensing Symposion (IGARSS)*, Seoul, ROK, 2005.

[3] K. A. C. de Macedo, R. Scheiber, and A. Moreira. An autofocus approach for residual motion errors with application to airborne repeat–pass SAR interferometry. *IEEE Transactions on Geoscience and Remote Sensing*, 2007. under review.

[4] R. F. Hanssen. *Radar Interferometry: Data Interpretation and Error Analysis*. Kluwer Academics, 2001.

[5] A. Moreira and Y. Huang. Airborne SAR processing of highly squinted data using a chirp scaling approach with integrated motion compensation. *IEEE Geoscience and Remote Sensing*, 32:1029–1040, 1994.

[6] P. Prats, A. Reigber, and J. Mallorqui. Interpolation-free corgistration and phase-correction of airborne SAR interferograms. *IEEE Geoscience and Remote Sensing Letters*, 1(3):188–191, 2004.

[7] H. A. Zebker, P. A. Rosen, and S. Hensley. Atmospheric effects in interferometric synthetic aperture radar surface deformation and topgraphic maps. *Journal of Geophysical Research*, 102:7547–7452, 1997.